Formation of highly adherent nano-porous alumina on Ti-based substrates: a novel bone implant coating

E. P. BRIGGS, A. R. WALPOLE, P. R. WILSHAW*
Department of Materials, University of Oxford, Parks Road, Oxford OX1 3PH, UK
M. KARLSSON*, E. PÅLSGÅRD
Center For Surface Biotechnology, BMC, Husarg. 3, D7:3, Box 577, 751 23, Uppsala, Sweden
E-mail: marjam.karlsson@ytbioteknik.uu.se

Thin, nano-porous, highly adherent layers of anodised aluminium formed on the surface of titanium alloys are being developed as coatings for metallic surgical implants. The layers are formed by anodisation of a 1–5 μm thick layer of aluminium which has been deposited on substrate material by electron beam evaporation. The surface ceramic layer so produced is alumina with 6–8 wt % phosphate ions and contains $\sim 5 \times 10^8\,cm^{-2}$ pores with a ~ 160 nm average diameter, running perpendicular to the surface. Mechanical testing showed the coatings' shear and tensile strength to be at least 20 and 10 MPa, respectively. Initial cell/material studies show promising cellular response to the nano-porous alumina. A normal osteoblastic growth pattern with cell number increasing from day 1 to 21 was shown, with slightly higher proliferative activity on the nano-porous alumina compared to the Thermanox control. Scanning electron microscopy (SEM) examination of the cells on the porous alumina membrane showed normal osteoblast morphology. Flattened cells with filopodia attaching to the pores and good coverage were also observed. In addition, the pore structure produced in these ceramic coatings is expected to be suitable for loading with bioactive material to enhance further their biological properties.

1. Introduction

Approximately 200 000 hips are replaced each year in the United States alone and as life expectancy and the activity levels of an ageing population increase [1] this number will continue to grow [2]. At present, most replacements are performed using cemented designs. However, despite their success and popularity there are still significant problems associated with their use. After 15 years of post-operative use, 15–25% of devices have failed requiring costly and traumatic revision surgery [2]. Implant loosening is evident in 20% of cases by five years post-operatively and 30% by 10 years [3] and is commonly associated with failure occurring because of inadequate bonding between implant and bone.

To overcome this problem attempts have been made to produce cementless implant designs in which the implants are coated with bioactive ceramic materials such as hydroxyapatite and bioglass thereby allowing direct bonding between the coating and the bone [4]. Higher interfacial stiffness and strength is achieved with a direct bond between bone and bioactive material than is achieved through the fibrous interface that forms between bone and non-bioactive materials [5, 6]. However, to date such implants have had only limited success because either the hydroxyapatite itself is weak [7] or it is inadequately bonded to the metallic implant [7–10]. In each case, the problem of the generation of wear particles stimulating aseptic loosening and/or resorption as a result of immune response [11] and the consequent failure of the implant still arises. Cementless designs have also been developed where bone attachment is achieved mechanically by bony in-growth into pores of 100–400 μm diameter formed in metallic coatings. However, in this case there are problems associated with the strength of the porous material [8]. Porous implants and implant coatings have a high surface area which may facilitate the leaching of ions from the implant into the body [12]. Currently, cementless implants have no better long-term survivability than cemented [13].

There is thus a need to produce non-metallic coatings on metallic implant materials with improved mechanical properties and bioactivity sufficient to promote bone adhesion so that micro-movements are suppressed. Titanium and its alloys as the most biocompatible metallic biomaterials [14–17], and having elastic modulus most similar to bone of all metals [16, 17] are ideal substrate materials for the coating.

*Author to whom all correspondence should be addressed.

Anodisation is a widely used commercial process and is a low cost method of producing corrosion resistant aluminium parts [18, 19], such as window frames. It has the effect of covering the metallic aluminium with a strongly adherent surface layer principally composed of ceramic alumina (Al_2O_3). Anodisation is carried out at, or near, ambient temperatures, in contrast to many of the present methods of producing ceramic coatings on implant materials which often deposit the coating at high temperature (e.g. plasma spraying) or require a high temperature densification stage (e.g. electrophoretic deposition). Low temperature processing is desirable since it avoids problems associated with differences in thermal expansion of the substrate and coating which can lead to the cracking of the coating with a consequent loss of mechanical properties [7]. High temperatures can also degrade the mechanical properties of the implant material by phase transformation and grain growth [7]. Alumina has proved successful as a dental and orthopaedic implant material [20, 21] and has excellent biocompatibility and corrosion resistance [22, 20]. Alumina has also been used coated with HA and bioglass [23–28] for example, for hip replacement.

In the present work, we have used a simple deposition and anodisation process to produce a highly adherent, nano-porous alumina coating on titanium alloy implants. In addition, primary human osteoblast-like (HOB) cells were cultured on alumina membranes with similar chemical composition and surface morphology to the coating in order to determine how bone cells are likely to respond to the implant coatings.

Nano-porous alumina coatings formed by anodisation, similar to those studied here, are also under investigation as a new generation of implants for radiotherapy and drug delivery. In particular, this technology is being developed for implants such as stents to deliver local radiotherapy to surrounding soft tissue using radioactive molecules bound into the pores of the alumina coating [29].

2. Materials and methods

2.1. Anodised aluminium

The anodised aluminium layers used in the present work are typical of those produced when aluminium is anodised in certain acid electrolytes. Under these conditions a porous surface layer of oxide is formed. The pores in the oxide layer are roughly cylindrical and are often arranged in an approximately hexagonal close packed array such that each pore extends from the surface of the oxide layer towards the underlying aluminium [30]. The pores are roughly parallel to each other and run perpendicular to the layer surface. At the base of each pore is a thin barrier layer of oxide separating the pore from the metallic aluminium underneath, see Fig. 1. As the anodisation process continues, oxidation of the aluminium occurs at the boundary between the oxide and the aluminium and is accompanied by electric field enhanced dissolution of the oxide layer at the base of each pore. In this way, the pores get longer and the porous film thicker as the remaining metallic aluminium is gradually thinned. The porous oxide layer so produced is not pure alumina (Al_2O_3) but

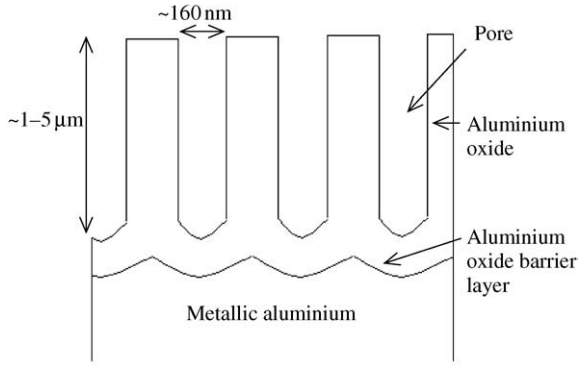

Figure 1 A schematic cross-sectional diagram of the structure of porous anodised aluminium.

contains some of the ions present in the electrolyte used for the anodisation [31, 32]. It is found that the porous films produced are highly hydrophilic, show low protein binding and are stable in most liquids with pH in the range 3–9.5 (see for example, 33).

For some metals, including Ti and some titanium alloys, anodisation usually results in the growth of a dense, non-porous, oxide layer. As the anodisation process progresses on these metals the oxide layer thickens and ion transport through it slows until the layer is so thick that further oxidation effectively stops. Anodisation of Ti–6Al–4V has been shown to increase its corrosion resistance in a physiological solution simulating the environment in the human body [34] by creating a thick oxide film on the surface. In the present work, phosphoric acid was used as the electrolyte allowing anodisation to be carried out at high voltages without excessive current flow and heat evolution [35]. This anodisation produces larger diameter pores than is possible using other electrolytes. Under these conditions, the alumina contains 6–8 wt % phosphate ions [31] and the phosphate ion distribution is such that the pore walls are relatively rich in phosphate while the alumina regions away from the pore walls are relatively pure [36].

Two different types of anodised aluminium layers were used for experimental characterisation in this work. The first were prepared directly on titanium alloy substrates and were used to test the mechanical properties of the layers and their attachment to the substrates. The second were freestanding alumina membranes obtained from Whatman, Maidstone, Kent, England which were used to determine cell response. For both types of anodised aluminium layers, the anodisation procedure was carried out at 160 V in phosphoric acid (0.4 M) to produce pores $\sim$ 160–200 nm diameter. In each case the production of the porous layer proceeds by anodisation occurring at the interface between a pure Al layer and the electrolyte. Since the anodisation conditions and electrolyte were the same during the production of the membranes and during the anodisation of the coatings it is expected each will have similar chemical composition and that similar cell behaviour will be found on the nano-porous Al_2O_3 surface coatings compared to the free standing membranes. However, it should be noted that the anodisation process used to produce the membranes, which are 60 μm thick, takes longer than that for the coatings of thickness 1–5 μm. This extra processing time results in the pores in the membrane

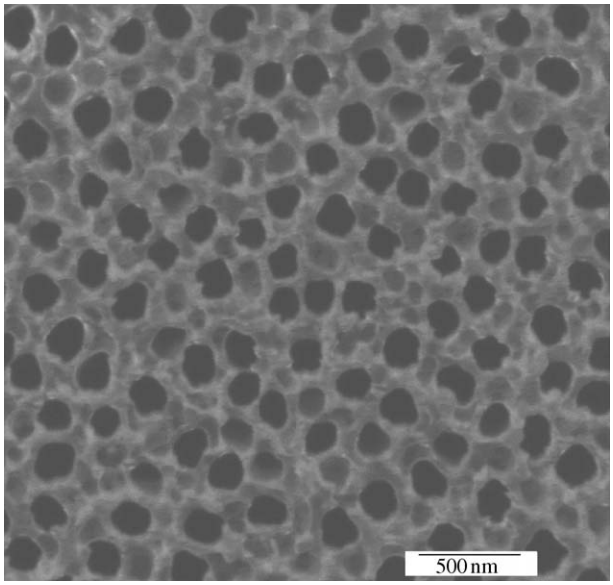

Figure 2 SEM micrograph of a commercial anodised aluminium oxide membrane used for the cell culture experiments.

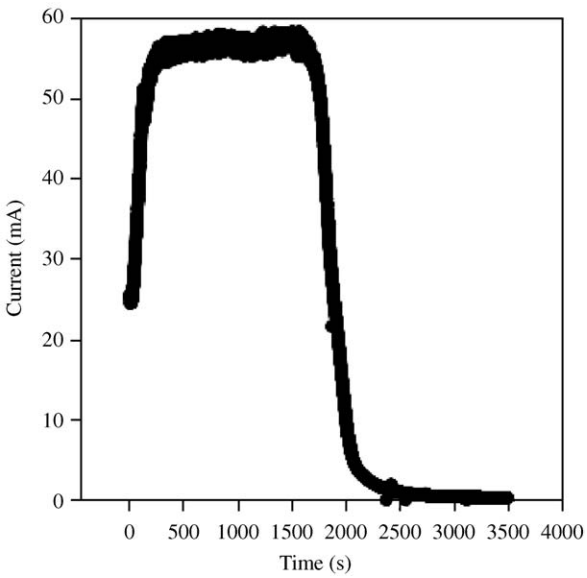

Figure 3 Anodisation current *vs.* time for 1260 mm^2 of Al deposited onto a pure Ti substrate and exposed to 0.4 M phosphoric acid.

having diameters of approximately 200 nm whereas in the coatings they are $\sim$ 160 nm. Fig. 2 shows the surface topography of an alumina membrane.

2.2. Specimen preparation

Anodised aluminium layers were produced on substrates of the titanium alloy Ti–6Al–4V and also on pure Ti. These substrates were chosen since they are used in the manufacture of surgical implants. The samples were prepared according to the following procedure.

2.2.1. Production of aluminium layers

Discs with a diameter of 20 mm were cut from 2 mm thick Ti–6Al–4V sheet. The discs were then polished to a mirror finish on one side using 6 μm diamond paste and then thoroughly cleaned, dried and rinsed in acetone. An Edwards Coating System E306A electron beam evaporator was used to deposit aluminium layers 1–5 μm thick on the polished surfaces while the specimens were held under vacuum at either room temperature or 300 °C. The beam voltage was 5 kV and deposition rates of approximately 1 nm s^{-1} were used.

2.2.2. Anodisation

Samples coated with aluminium layers were prepared for anodisation by making electrical contact to the backside of the discs. The specimens were then mounted in a reaction vessel such that a 1260 mm^2 area of the aluminium layer was exposed to the electrolyte and subsequently anodised. Anodisation was carried out in 0.4 M phosphoric acid electrolyte held at 15 °C and the applied voltage was ramped up to 160 V starting at 10 V and increasing by 4 V every 5 s. The voltage was gradually increased in this way to prevent electrical breakdown of the oxide. Prevention of oxide breakdown was also aided by maintaining vigorous stirring throughout the course of the experiment. The inter-electrode distance was 70 mm. When using phosphoric acid electrolyte it has been reported [37] that the pore diameter increases by 1 nm for every volt applied and the cell spacing increases by 2.5 nm per volt. Thus for the anodising voltage of 160 V used in this work, the pore diameters were $\sim$ 160 nm with a corresponding pore density of $\sim 5 \times 10^8$ cm^{-2} as measured by SEM.

The applied potential and resulting current were controlled and monitored by computer. The 160 V anodisation potential was maintained until the anodising current had dropped to a sufficiently low value, usually less than 1 mA cm^{-2}, which is typical of the anodisation of uncoated Ti–6Al–4V substrates, Fig. 3. At this point, it was assumed that all the aluminium had been anodised and the anodisation process was stopped.

Additionally, pure Ti, Ti–6Al–4V, 316L stainless steel, and cobalt chrome alloy substrates not covered with a layer of aluminium were also exposed to this same anodisation procedure for comparison.

2.3. Mechanical properties

In order for the shear and tensile strength of the coatings to be measured, well defined areas of coating were glued onto steel test pieces and tested to failure at a constant strain rate of 6 mm/min, using a Mayes DM30 tensile test machine fitted with a Rubicon digital control system. The adhesive used was EPX 37/50 available from 3M. Standards have been developed for testing the mechanical properties of coatings in both shear and tension (ASTM F1044-95 and ASTM F1147-99). These were followed here with the exception that in the present work the coating area tested in tension was 2.41 cm^2 instead of 5.07 cm^2. The coating areas tested in shear were $\sim$1.7 cm^2.

2.3.1. Mechanical testing

Mechanical testing was performed on alumina layers fabricated on Ti–6Al–4V substrates. For tests of the coating shear strength, the specimens were cleaned using acetone and glued to a steel backing plate.

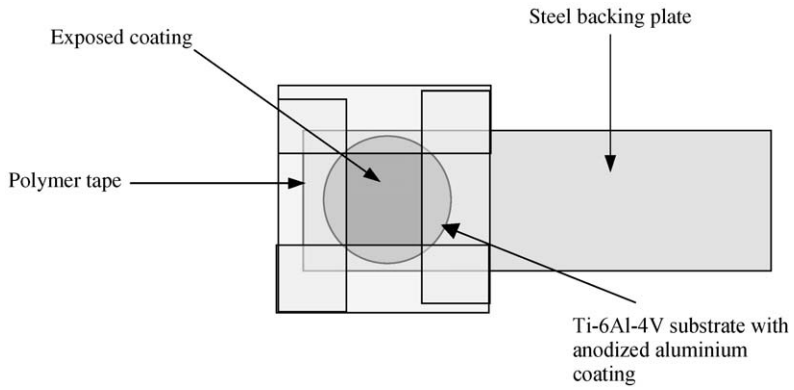

Figure 4 Definition of the sample area to be tested in shear strength mode.

The area of coating to be tested was defined by applying weakly adhering tape to the surface of the coating as shown in Fig. 4. It was assumed that the adherence of the tape to the coating and of the adhesive to the tape was sufficiently poor as to have a negligible effect on the measured failure stress of the sample.

A test plate of similar dimensions to the backing plate was then glued to the exposed coating to form the test structure. Shear testing was performed using the set up shown in Fig. 5.

A test rig as shown in Fig. 6 was used for tensile testing. The alumina surface was cleaned in acetone before gluing to the test plate. The area over which the coating was tested in tension was controlled by the test plate diameter.

2.4. Cells and culture conditions

Human osteoblast-like cells originally isolated from femoral head trabecular bone fragments were cultured in Dulbecco's modified Eagles medium (DMEM) supplemented with 10% foetal calf serum (FCS), 1% non-essential amino acids, L-ascorbic acid $(150\,\mathrm{g\,ml^{-1}})$, 0.02 M L-glutamine, 0,01 M HEPES, $100\,\mathrm{units\,ml^{-1}}$ penicillin and 100 µg streptomycin at 37 °C, 5% CO_2 in a humidified atmosphere [38].

When cell attachment experiments were to be performed, cells were harvested by trypsin-EDTA treatment, collected by centrifugation and resuspended in DMEM supplemented with the above. The cells were counted using a hemacytometer and the cell concentration calculated. Approximately 100 000 cells for the biochemical study and 10 000 for the morphological study, were then seeded on to porous alumina membranes and a control Thermanox (TMX, Life Technologies) surface. The membranes, provided by Whatman were 60 µm thick and the pores $\sim$ 200 nm in diameter on one side and $\sim$ 20 nm in diameter on the other. Care was taken to expose the cells to the side with the $\sim$ 200 nm pores. The membranes were placed in 24-well tissue culture polystyrene plates (NUNC) and cultured for up to three weeks. Triplets of each membrane per timepoint were used.

2.4.1. Biochemical analysis

Cell attachment and proliferation was determined by using Alamar Blue [39].

Alamar Blue is a non-toxic metabolic indicator of viable cells, that is, when taken into cells, the dye is reduced and both fluoresces and changes colour. Thus the amount of colour/fluorescence developed correlates with the amount of living cells in the sample.

The medium from all wells was removed after 1, 3, 7, 14 and 21 days and substituted with 10 × Alamar Blue stock solution (Serotec) in phenol free medium. The

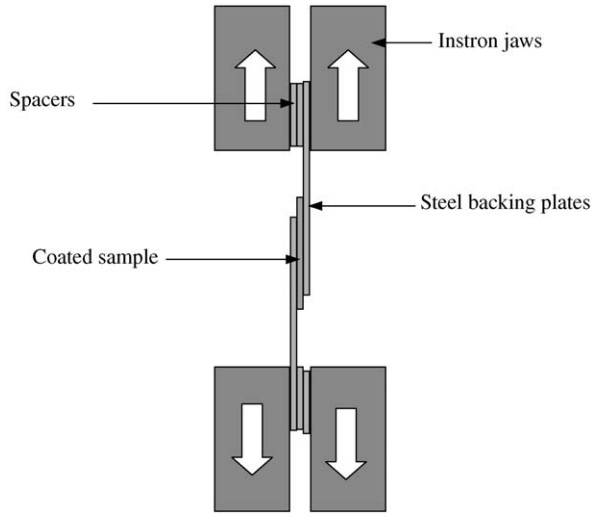

Figure 5 The experimental set up for shear strength testing of coatings.

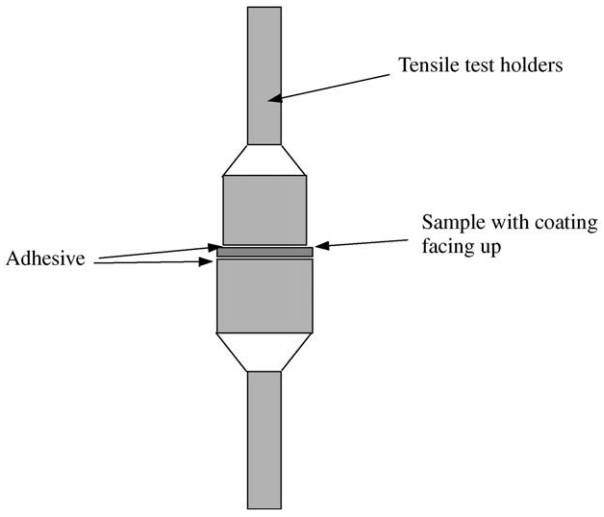

Figure 6 The experimental set up for tensile strength testing of coatings.

plates were then incubated at 37 °C, 5% CO_2 in a humidified atmosphere for 3 h. Aliquots of 100 µl from each well were then transferred to a 96-well plate and the fluorescence ($\lambda_{ex} = 560$ nm, $\lambda_{em} = 590$ nm) was read. All values were corrected for background fluorescence of reagent with substrate without cells. To continue culturing the cells, the remaining Alamar Blue was removed from the 24-well plates, replaced with fresh culture medium and returned to the incubator.

2.4.2. Microscopic analyses

Cells were fixed with 1.5% glutaraldehyde after 1, 3 and 7 days of incubation. The cells were then stained in 1% osmium tetroxide and 1% tannic acid, then dehydrated through a series of alcohol concentrations (20, 30, 40, 50, 60 and 70%), stained in 0.5% uranyl acetate (in 70% alcohol), and then dehydrated further (90, 96 and 100% alcohol). The final dehydration was done in hexamethyldisilazane, followed by air-drying. The samples were then coated with gold and examined using a Jeol SEM.

3. Results

3.1. Anodisation behaviour

Six different types of specimens were subjected to the anodisation treatment. For the 316L stainless steel and the cobalt chrome alloy specimens, it was found that as the anodising voltage was increased so the anodising current also rapidly increased. No stabilisation or subsequent reduction in the magnitude of the anodisation current was observed. This behaviour indicates a vigorous reaction taking place and that no stable anodic film was generated on these metals in the electrolyte used.

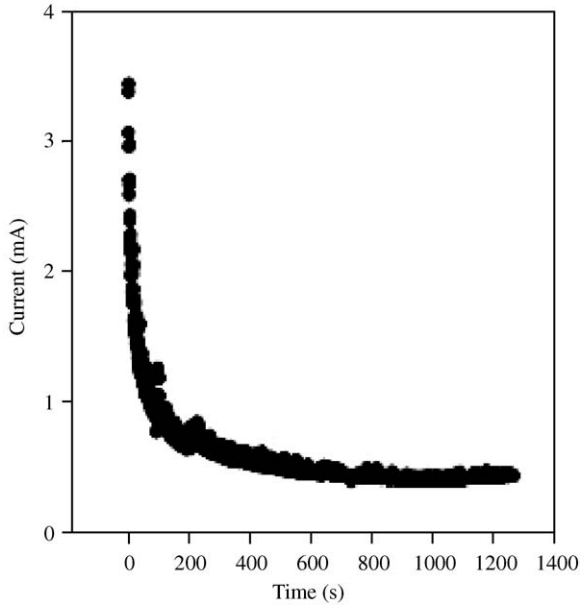

Figure 7 Anodisation current *vs.* time for 1260 mm^2 of Ti–6Al–4V exposed to 0.4 M phosphoric acid.

For the uncovered pure Ti and Ti–6Al–4V substrates and also for those with the surface aluminium layer, the behaviour of the anodisation current *vs.* voltage with time indicated that stable anodic oxide films were being produced. Fig. 7 shows the curves for the Ti–6Al–4V alloy with similar results (not shown here) being obtained for the pure Ti specimens. Fig. 7 shows the anodising current decreasing with time as the dense, non-porous, barrier oxide layer on the surface of the Ti–6Al–4V alloy gradually thickened. After 600 s the barrier layer was sufficiently thick that further anodisation had practically stopped and the current had fallen below 0.4 mA cm^{-2}. Fig. 3 shows anodisation current vs. time for a Ti layer covered with aluminium. The anodisation current increased rapidly for the first $\sim$ 190 s as the voltage was increased from 0 to 160 V. After this time some further increase in current was detected as a stable pore structure developed in the anodic film. From $\sim$ 300 to $\sim$ 1800 s the anodisation current remains stable as the aluminium layer was gradually anodised to form the porous anodic oxide layer. In this time, the thickness of the porous layer increases as the aluminium layer is gradually oxidised. After $\sim$ 1800 s the current decreased rapidly towards zero in a manner characteristic of the anodisation of the underlying Ti layer. Our interpretation of this behaviour is that the steady state condition of stable and continuous anodisation of the aluminium layer (between $\sim$ 300 and $\sim$ 1800 s) continues until the advancing alumina/aluminium interface reaches the titanium substrate. At this point (time $\sim$ 1800 s) the dense non-porous oxide layer starts to form on the surface of the Ti and the current rapidly decreases. After approximately a further 300 s the anodisation behaviour is typical of that of a Ti substrate indicating that all the surface aluminium has been converted to alumina and the specimen is now behaving, from an electrical point of view, as if it were uncoated Ti. Similar data were obtained from aluminium layers deposited on both Ti and Ti–6Al–4V alloy layers.

3.2. Coating morphology

When the aluminium was deposited on the polished substrates at room temperature the result was a surface layer with a mirror finish. After anodisation this produced a porous layer with a smooth surface. However, mechanical measurements (see later) on such specimens showed poor adhesion between the alumina layer and the underlying substrate.

Further experiments were performed depositing the aluminium on substrates which were held at 300 °C *in situ*. Under these conditions the deposited layers had a cloudy appearance indicating that they were no longer smooth. Optical microscopy showed this to be due to the growth of individual aluminium grains within the layer leading to surface roughening. Fig. 8(a) shows the surface topography of such a specimen after subsequent anodisation.

The micron scale roughness evident in the alumina film shown in Fig. 8(a) is due to the surface roughness of the aluminium layer before anodisation. At a smaller scale, see Fig. 8(b), pores of $\sim$ 160 nm diameter can be

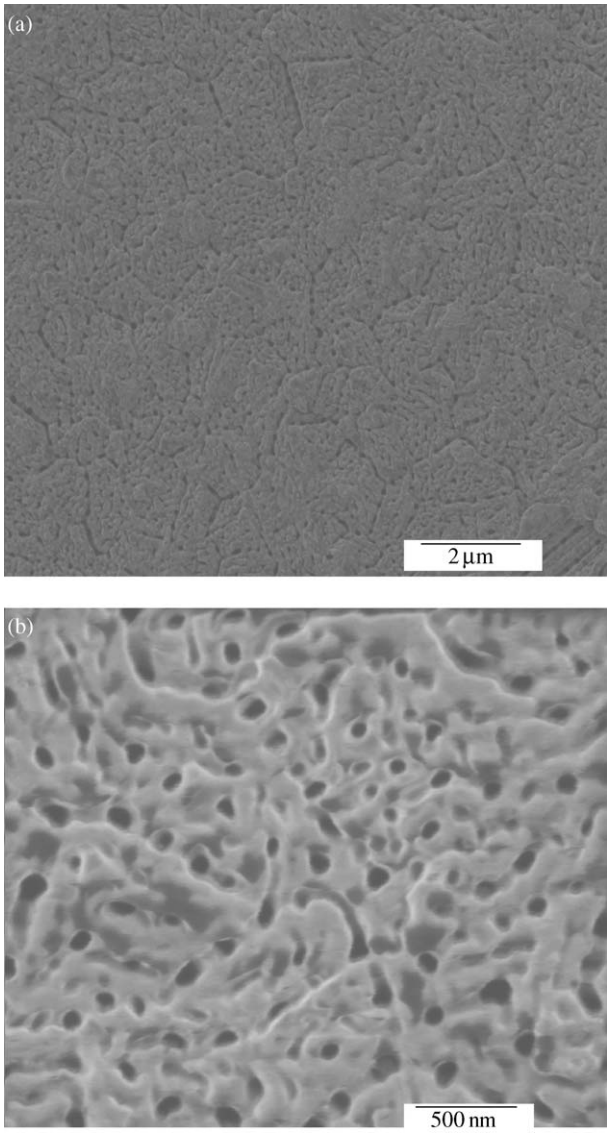

Figure 8 (a) SEM micrograph of an anodised aluminium layer (alumina) formed from anodisation of aluminium deposited at 300 °C onto a Ti–6Al–4V substrate. Surface roughness due to grains in the layer is visible. (b). High resolution SEM micrograph of an anodised aluminium layer, as for Fig. 8(a), showing the individual pores (~ 160 nm) present in the material.

observed. The topography of this specimen is considerably less regular and much rougher than that generally associated with anodised aluminium, see, for example, Fig. 2. The adhesion of the layers deposited at 300 °C was, however, good and it was these layers, after anodisation, that were used for subsequent mechanical testing.

3.3. Mechanical properties

All mechanical measurements were carried out on anodic alumina layers prepared on Ti–6Al–4V alloy substrates for which the aluminium had been deposited at 300 °C. A total of 16 specimens were tested either in shear or tension. Only one failure of the test piece was due to failure of the alumina layer rather than the adhesive. For the shear measurements the highest stress applied before glue failure was 20.4 MPa with the average being 13.5 MPa. In tension, the highest load to failure was 10.0 MPa with the average being 3.5 MPa. In only one case did the alumina layer fail in tension at a stress of 3.5 MPa. SEM examination showed that this failure occurred at the interface between the polished Ti–6Al–4V substrate and the surface alumina layer. Thus, in all but one of the samples the coating did not fail, instead the failure of the test structure was due to the failure of the adhesive.

3.4. Cell behaviour

3.4.1. Biochemical analysis

The Alamar Blue analysis showed a normal osteoblast growth pattern with REDOX reactions (and hence cell number) increasing from day 1 to 21, see Fig. 9. One can also see a small but statistically significant increase in the proliferative activity of the HOB cells on the nanoporous alumina compared to the Thermanox material used as a control.

3.4.2. Microscopic analyses

Scanning electron microscopy (SEM) examination of HOB cells on the porous alumina membranes showed normal osteoblast morphology. One could observe flattened cells with processes showing some evidence for attachment to the pores of the material as shown in Fig. 10. Good cell coverage was also observed.

4. Discussion

4.1. Anodisation

The anodisation experiments showed that layers of anodised aluminium could be produced directly bonded

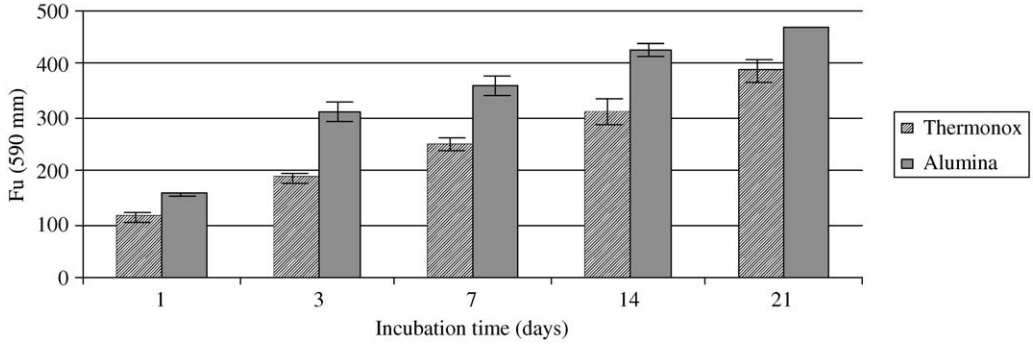

Figure 9 Graph demonstrating the proliferation of HOB cells in culture for 1, 3, 7, 14 and 21 days on porous alumina compared with a control as determined by Alamar Blue assay. (Each value represents the mean of three samples.)

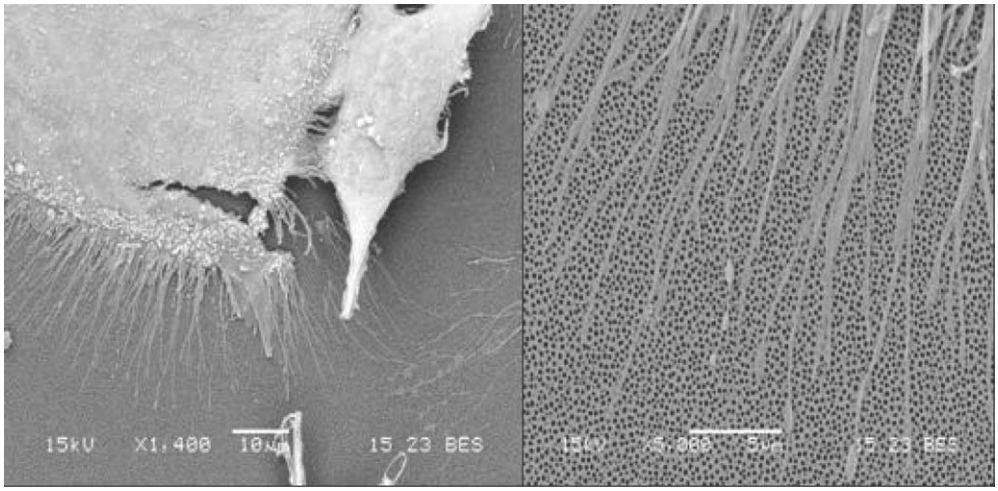

Figure 10 Scanning electron micrographs of fixed HOB cells cultured on nano-porous alumina membranes. (a) micrograph after 24 h in culture, (b) as micrograph (a) but at higher magnification, showing some evidence for filipodia attachment to pores.

to pure Ti or Ti–6Al–4V substrates. However, when attempts were made to anodise 316L stainless steel and cobalt chrome alloy specimens in the phosphoric acid electrolyte a rapid reaction took place. This indicated that these metals are unsuitable for the present process because it would not be possible to completely anodise an aluminium layer deposited on top of them without experiencing a vigorous reaction when the electrolyte reached the underlying substrate towards the end of the anodisation procedure.

Implants made of such alloys might still be covered with a layer of porous alumina using anodisation but it would be necessary either to deposit a barrier layer of a material such as titanium between the substrate and aluminium layer or not to anodise completely the surface aluminium layer. In either case, the electrolyte would not reach the underlying reactive substrate and an intact adhered surface alumina layer could still be produced.

4.2. Mechanical properties

The layers deposited at room temperature were only weakly bonded to the underlying substrate and would therefore be unsuitable for use as an implant coating. It is likely that the weak adherence of these layers was due to a residual layer of organic residue between the substrate and deposited aluminium layer or due to the thin native oxide present on the Ti or Ti–6Al–4V alloy substrates. In any case, the interlayer would have prevented direct contact and hence bonding between the metal substrate and deposited aluminium layer so resulting in a weak interface. The effect of heating the substrate can then be understood in terms of removing any organic material present and/or causing diffusion through, and break up of, the native oxide. The result is a strong bond between the surface aluminium and underlying metal substrate. Indeed, we believe it likely that the one specimen for which the coating failed during mechanical testing was probably inadequately cleaned before the aluminium layer was deposited and that an improved surface preparation procedure will overcome this problem thereby allowing strongly adhered coatings to be prepared using aluminium deposited at room temperature.

The mechanical measurements of the coatings made from aluminium deposited onto the Ti–6Al–4V alloy specimens at 300 °C were limited by the strength of the adhesive used. For every specimen except one, failure was due to the glue rather than the coating. Since a failure either within the alumina layer itself or at the interface between the alumina and substrate would have been detected these results imply that the implant coatings are likely to withstand stresses in excess of 20 MPa in shear and 10 MPa in tension. For comparison, the shear strength of bovine cortical bone has been measured to be 34 MPa [7] and previously published data for the shear strength of HA deposited on polished Ti–6Al–4V surfaces was found to be $\sim$ 12 MPa [7]. Furthermore, it is possible to roughen the surface of the implant material prior to aluminium deposition so increasing its surface area. This is expected to increase the effective coating/substrate interface strength both in shear and tension.

The results presented here indicate that the process of producing a surface alumina layer on implant material by anodisation promises to yield a surface ceramic coating with shear strength similar to that of the bone in which it might be implanted.

4.3. Cell behaviour

Promising cellular response was shown when HOB cells were cultured on porous alumina membranes. The material is able to support normal osteoblastic cell growth with cells rapidly spreading on the surface. SEM examination of HOB cells on the membranes showed normal osteoblast morphology. Flattened cells were observed with processes which looked in some cases to be attached to the pores of the material. This may lead to the cells anchoring efficiently to the porous surface and therefore adhering better than on a dense material.

The fact that the phosphate ion distribution is such that the pore walls contain higher concentration of phosphate than the rest of the membrane structure [36] should lead to a high concentration of phosphate ions in the local cellular environment. This may be beneficial for the mineralisation. However, it should be noted that this characterisation of cell behaviour was performed on the

free standing anodic aluminium oxide membranes whereas the substrate coatings used for mechanical testing were produced by anodisation of an aluminium layer bonded to the substrate material. Thus the cell data presented here will only give an indication of how HOB cells will behave on the actual substrate coatings, although as noted previously it is expected that their behaviour will be similar in each case.

Most orthopaedic surgery leads to unavoidable bone cell death at the implant site. Remodelling of bone should eventually occur but any stimulus or factor that could improve the initial healing would be advantageous. The fact that the anodised aluminium material also has the potential of being rendered bioactive by loading the porous structure with appropriate bioactive agents might improve the cell response and facilitate osseoinductive activity.

5. Conclusions

This investigation has shown that nano-porous alumina coatings can be made successfully on Ti and Ti–6Al–4V alloys. For the coating to be applied to stainless steel or cobalt chrome alloys an additional titanium layer would have to be applied prior to the aluminium, to protect the substrate alloy from the anodisation procedure.

The adhesion of the coatings made on Ti–6Al–4V has been tested in shear and tension. The results show that on a polished, smooth surface the coating has a shear strength likely to exceed 20 MPa and tensile strength likely to be greater than 10 MPa.

Encouraging cellular response was shown when HOB cells were cultured on porous alumina membranes similar to the coatings produced for mechanical testing. The membranes seem to be able to support normal osteoblastic cell growth with cells rapidly spreading and flattening on the surface of the material.

Acknowledgments

The authors thank Dr Lucy Di Silvio for her support and guidance and also for use of lab space and equipment and for supplying the cells. The authors would also like to thank Mr M Kayser and Dr R Langford for helping to prepare the micrographs. We are also indebted to The Swedish Foundation for International Cooperation in Research and Higher Education (STINT) for supporting this project.

References

1. T. KIRKWOOD, in ''Time of Our Lives'' (Weidenfeld and Nicholson, 1999).
2. L. L. HENCH, *MRS Bull.* **24** (1999) 13.
3. E. W. ABEL, in ''Hip Arthroplasty'' (Distance Learning Section, Department of Orthopaedic and Trauma Surgery, University of Dundee, 1997).
4. D. MUSTER, M. HAGE-ALI, K. T. RIE, T. STUCKY, A. CORNET and D. MAINARD, *MRS Bull.* **25** (2000) 25.
5. S. D. COOK, K. A. WALSH and R. J. HADDAD JR., *Clin. Orthop. Rel. Res.* **193** (1985) 271.
6. G. L. MAISTRELLI, N. MAHOMED, D. GARBUZ, FORNASIER, I. J. HARRINGTON and A. BINNINGTON, *J. Bone Joint Sur.* **74B** (1992) 452.
7. M. WEI, A. J. RUYS, M. V. SWAIN, S. H. KIM, B. K. MILTHORPE and C. C. SORRELL, *J. Mater. Sci.: Mater. Med.* **10** (1993) 401.
8. K. A. THOMAS, J. F. KAY, S. D. COOK and M. JARCHO, *J. Biomed. Mater. Res.* **21** (1987) 1395.
9. L. L. HENCH and O. ANDERSSON, in ''An Introduction to Bioceramics'', edited by L. L. Hench and J. Wilson (World Scientific Publishing Co. Pte. Ltd., Singapore, 1993) p. 239.
10. W. R. LACEFIELD, in ''Bioceramics. Material Characteristics vs. *In Vivo* Behaviour'', edited by P. Ducheyne and J. E. Lemons (The New York Academy of Science, New York, 1988) p. 72.
11. L. L. HENCH and E. C. ETHRIDGE, in ''Biophysics and engineering series'', Vol. 4 (Academic Press, New York, 1982).
12. B. M. WROBLEWSKI, P. D. SINEY and P. A. FLEMING, in ''Total Hip Arthroplasty Outcomes'', edited by G. A. M. Finerman, F. J. Dorey, P. Grigoris and H. A. McKellop (Churchill Livingstone, New York, 1998) p. 15.
13. L. L. HENCH and J. WILSON (eds.), in ''Clinical Performance of Skeletal Prostheses'' (Chapman and Hall, London, 1996).
14. M. NIINOMI, in ''Structural Biomaterials for the 21st Century'', edited by M. Niinomi, T. Okabe, E. M. Taleff, D. R. Lesuer and H. E. Lippard (TMS, 2001).
15. B. D. RATNER, in ''Titanium in Medicine'', edited by D. M. Brunette, P. Tengvall, M. Textor and P. Thomsen (Springer, Berlin, 2001) p. 2.
16. D. F. WILLIAMS, in ''Titanium in Medicine'', edited by D. M. Brinette, P. Tengvall, M. Textor and P. Thomsen (Springer, Berlin, 2001) Foreword VII–VIII, p. 14, p. 561.
17. L. L. HENCH, in ''Bioceramics-7'', edited by Ö. H. Anderson and A. Yli Urpo (Butterworth-Heinemann, Oxford, England, 1994) p. 3.
18. O. JESSENSKY, F. MULLER and U. GÖSELE, *J. Electrochem. Soc.* **145** (1998) 3735.
19. G. E. THOMSON, *Thin Solid Films* **297** (1997) 192.
20. S. F. HULBERT, in ''An Introduction to Bioceramics'', edited by L. L. Hench and J. Wilson (World Scientific Publishing Co. Pte. Ltd., Singapore, 1993) p. 25.
21. P. CHRISTEL, A. MEUNIER, J.-M. DORLOT, J.-M. CROLET, J. WITVOET, L. SEDEL and P. BOUTIN, in ''Bioceramics: Material Characteristics vs. *In Vivo* Behaviour'', edited by P. Ducheyne and J. E. Lemons (The New York Academy of Science, New York, 1988) p. 234.
22. L. L. HENCH, *J. Am. Ceram. Soc.* **74** (1991) 1487.
23. D. SHI and G. JIANG, *Mater. Sci. Eng.* **6** (1998) 175.
24. J. CAVLHEIRO and M. BRAS, *Bioceramics* **11** (1998) 65.
25. E. VERNÉ, C. VITALE BROVARONE, C. MOISESCU, E. GHISOLFI and E. MARMO, *Acta Materiala* **48** (2000) 4667.
26. M. HAMADOUCHE, A. MEUNIER, D. C. GREENSPAN, C. BLANCHAT, J. P. ZHONG, G. P. LA TORRE and L. SEDEL, *Key Eng. Mater.* **192** (2000) 413.
27. M. HAMADOUCHE, R. S. NIZARD, A. MEUNIER, C. BLANCHAT, P. MASQUELIER and L. SEDEL, in ''Bioceramics II'', edited by R. Z. Le Geros and J. P. Le Geros (New York, 1998) p. 427.
28. U. GROSS, H.-J. SCHMITZ and V. STRUNZ, in ''Bioceramics: Material Characteristics vs. *In Vivo* Behaviour'', edited by P. Ducheyne and J. E. Lemons (The New York Academy of Science, New York, 1998) p. 211.
29. T. SAWITOWSKI, W. BRANDAU, A. FISCHER, A. HEILMANN and G. SCHMID, *Mater. Res. Soc. Symp. Proc.* **581** (2000) 523.
30. G. E. THOMPSON and G. C. WOOD, in ''Treatise on Materials Science and Technology'', Vol. 23, edited by J. C. Scully (Academic Press, New York, 1983) p. 249.
31. G. E. THOMPSON, *Thin Solid Films* **297** (1997) 192.
32. C. ALVEY, PhD Thesis, University of Manchester (1978).
33. Whatman Data Sheet S9036–2092, in ''Anopore™ Inorganic Membranes'' (Whatman International Ltd., Maidstone, Kent, England).

34. A. CIGADA, M. CABRINI and P. PEDEFERRI, *J. Mater. Sci.: Mater. Med.* **3** (1992) 408.
35. R. C. FURNEAUX, W. R. RIGBY and A. P. DAVIDSON, *Lett Nature* **337** (1989) 147.
36. L. J. LANZEROTTI, W. L. BROWN, J. M. POATE and W. M. AUGUSTYNIAK, *Nature* **272** (1978) 433.
37. H. MASUDA, K. YADA and A. OSAKA, *Jap. J. Appl. Phys. Part 2 – Lett.* **37** (1998) 1340.
38. L. DI SILVIO, PhD thesis, University of London (1995).
39. G. R. NAKAYAMA, M. C. CATON, M. P. NOVA and Z. PARANDOOSH, *J. Immunol. Meth.* **204** (1997) 205.

Received 18 March 2003
and accepted 21 January 2004